Science Advances
AAAS

advances.sciencemag.org/cgi/content/full/6/18/eaax1346/DC1

Supplementary Materials for

Tumor microenvironment-activatable Fe-doxorubicin preloaded amorphous $CaCO_3$ nanoformulation triggers ferroptosis in target tumor cells

Chen-Cheng Xue, Meng-Huan Li, Yang Zhao, Jun Zhou, Yan Hu, Kai-Yong Cai, Yanli Zhao, Shu-Hong Yu*, Zhong Luo*

*Corresponding author. Email: shyu@ustc.edu.cn (S.-H.Y.); luozhong918@cqu.edu.cn (Z.L.)

Published 29 April 2020, *Sci. Adv.* **6**, eaax1346 (2020)
DOI: 10.1126/sciadv.aax1346

This PDF file includes:

Supplementary Materials

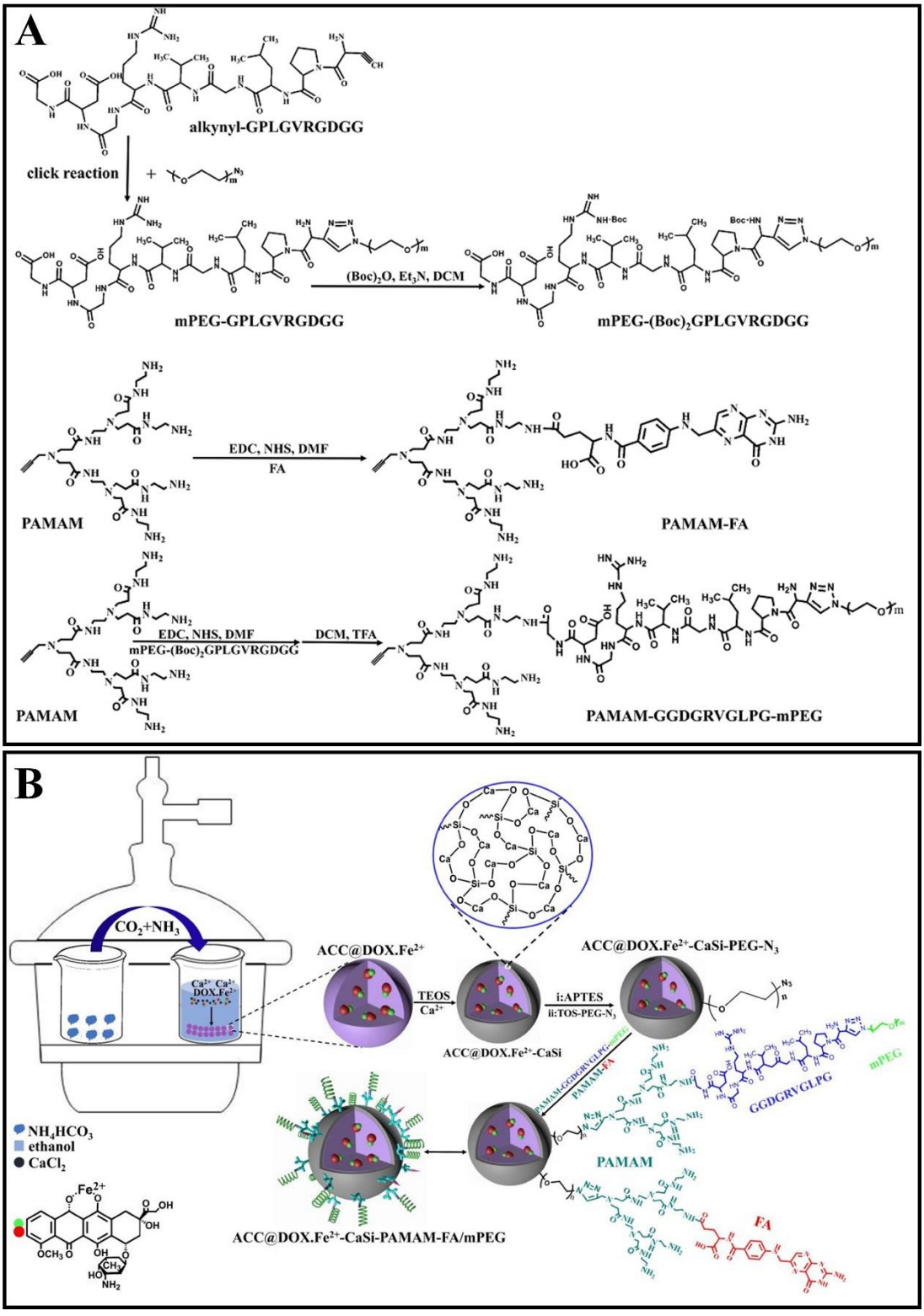

Fig. S1. Synthesis scheme for the key components of the ACC-based nanoformulation. A: The synthetic route of PAMAM-FA and PAMAM-GGDGRVGLPG-mPEG. B: The synthetic route of ACC@DOX.Fe^{2+}-CaSi-PAMAM-FA/mPEG.

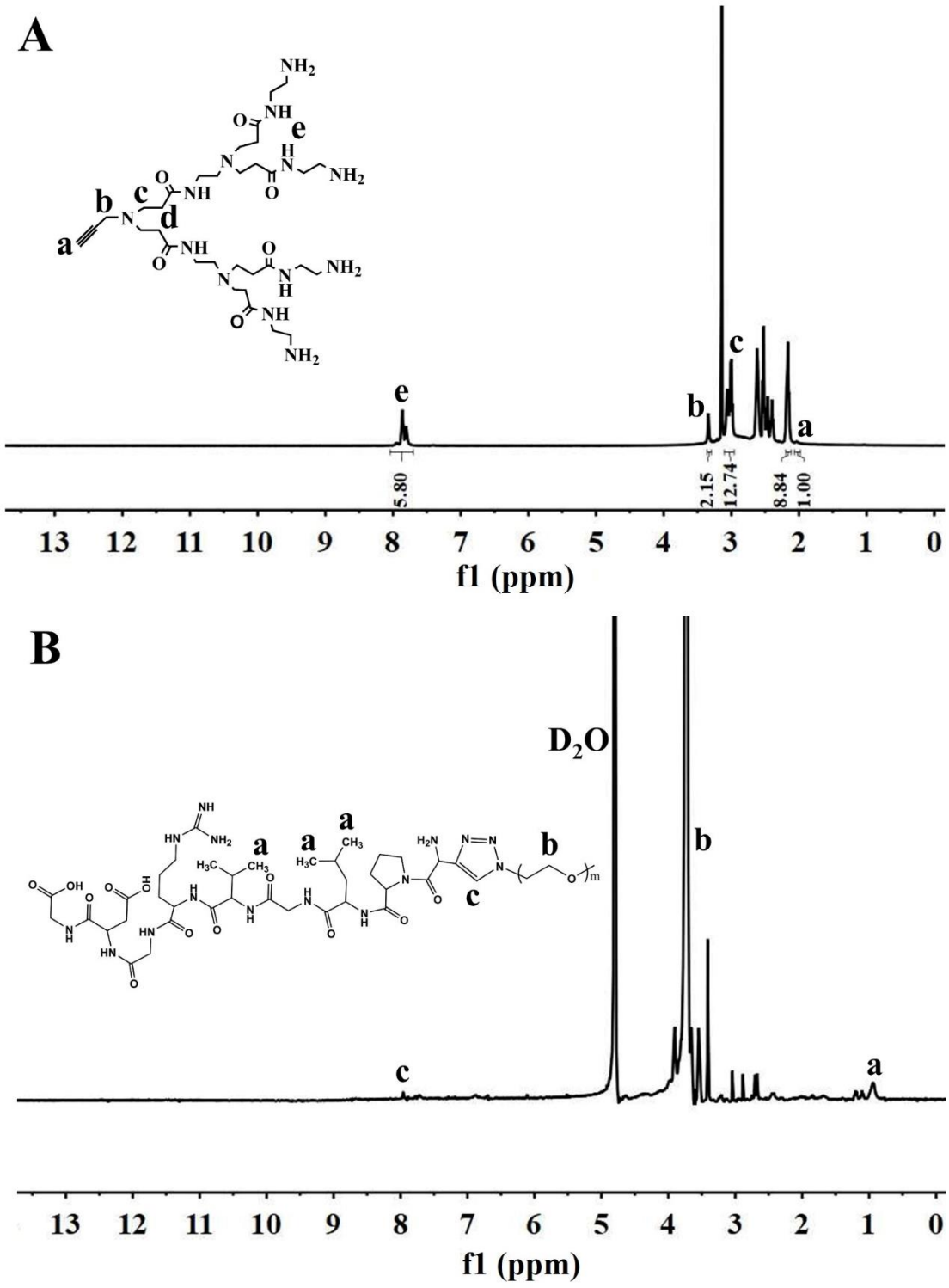
A
e
b
c
a
5.80
2.15
12.74
8.84
1.00
13 12 11 10 9 8 7 6 5 4 3 2 1 0
f1 (ppm)
B
D2O
b
c
a
13 12 11 10 9 8 7 6 5 4 3 2 1 0
f1 (ppm)

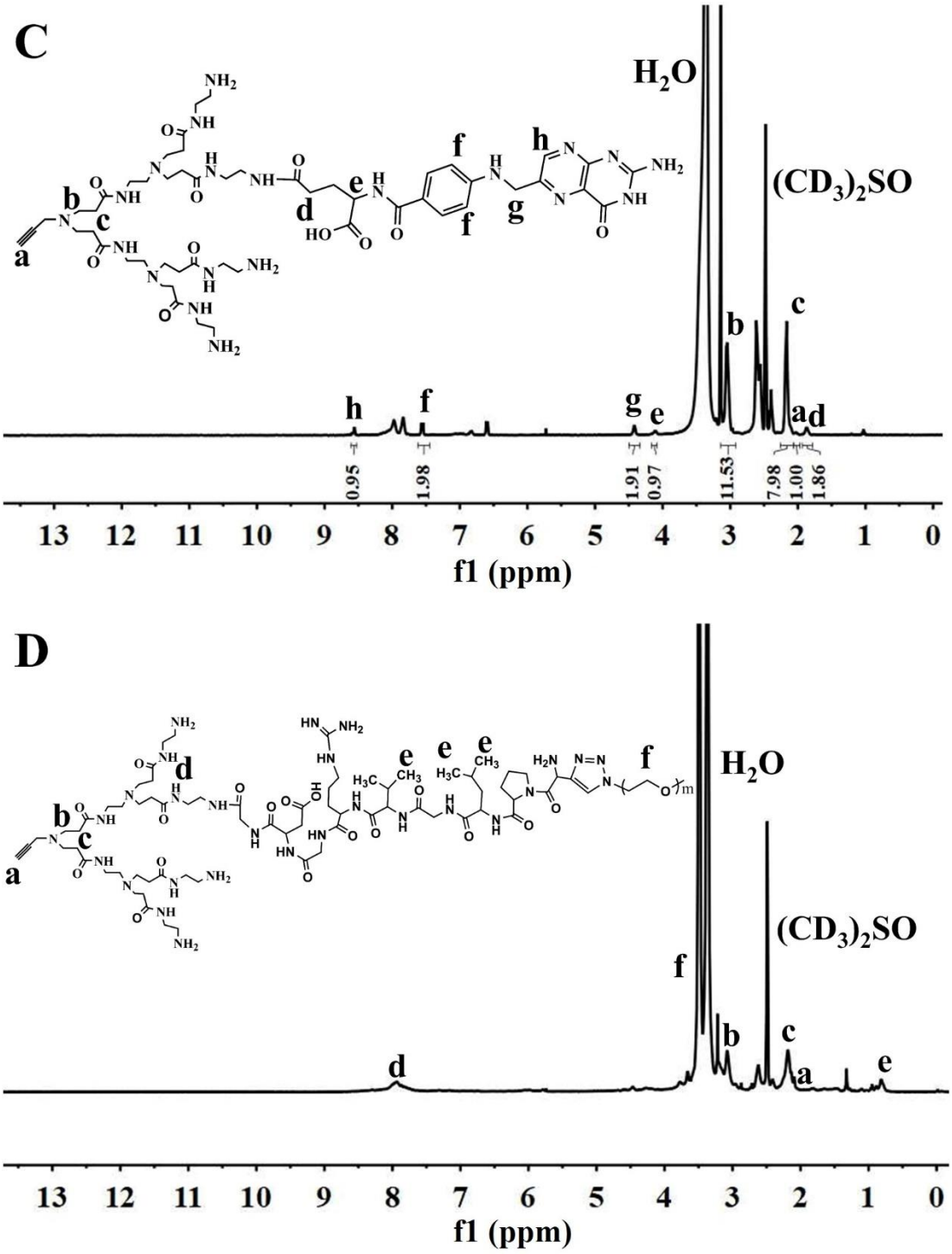

Fig. S2. NMR spectra of the key intermediate products. ^{1}H NMR spectra of (**A**): PAMAM, (**B**): mPEG-GPLGVRGDGG, (**C**): PAMAM-FA, (**D**): PAMAM-GGDGRVGLPG-mPEG.

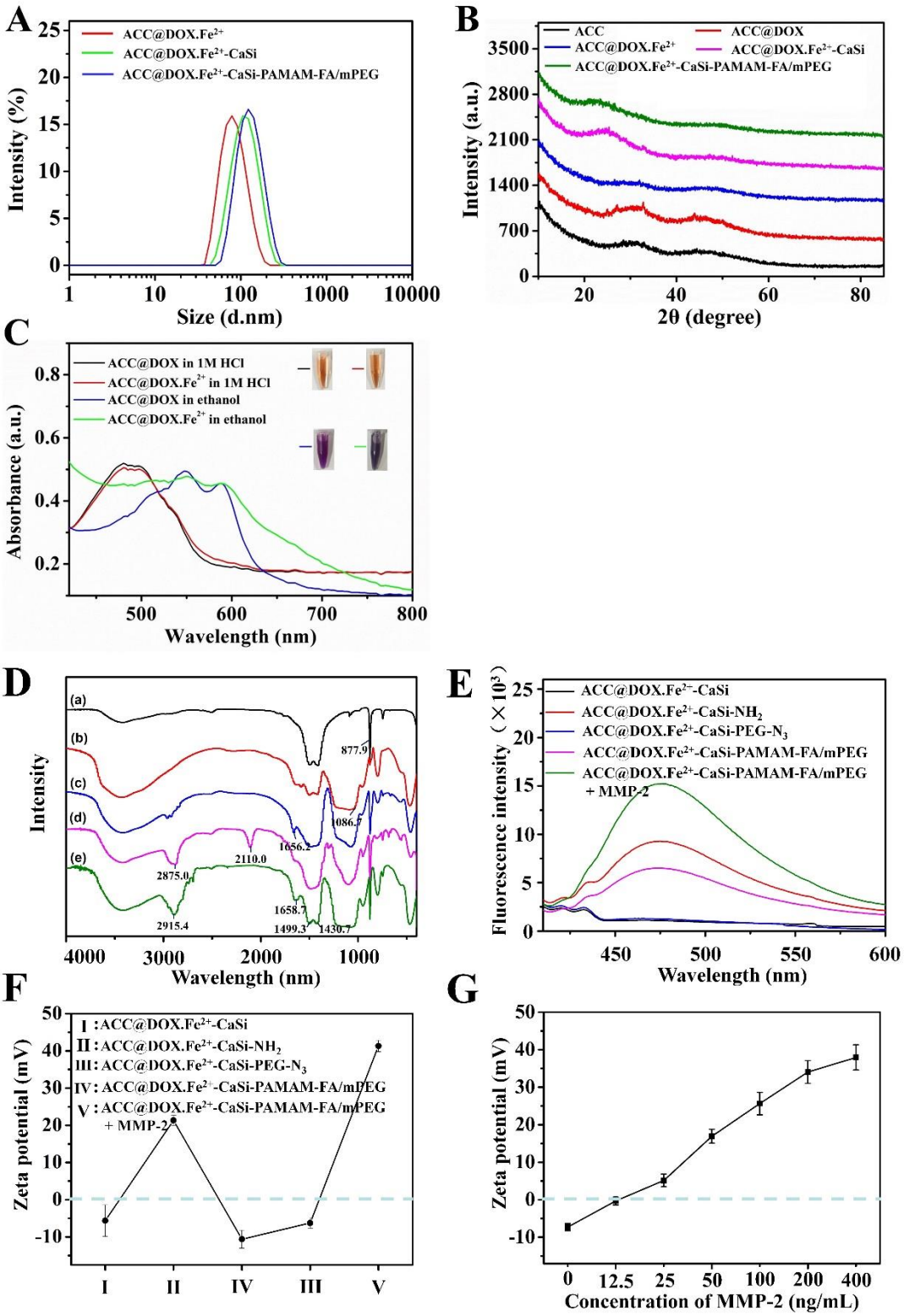

Fig. S3. Characterizations on the physical and spectroscopic properties of the nanoformulation as well as its MMP-2 responsiveness. A: The size distribution of ACC@DOX.Fe^{2+}, ACC@DOX.Fe^{2+}-CaSi and ACC@DOX.Fe^{2+}-CaSi-PAMAM-FA/mPEG were characterized by DLS. **B**: XRD analysis of ACC, ACC@DOX, ACC@DOX.Fe^{2+}, ACC@DOX.Fe^{2+}-CaSi and ACC@DOX.Fe^{2+}-CaSi-PAMAM-FA/mPEG. The missing peaks indicate that the nanoparticulate substrates are highly

amorphous. **C**: UV-vis spectra of ACC@DOX and ACC@DOX.Fe^{2+} dissolved in 1M HCl or ethanol. **D**: FTIR spectra of (a) ACC@DOX.Fe^{2+}, (b) ACC@DOX.Fe^{2+}-CaSi, (c) ACC@DOX.Fe^{2+}-CaSi-NH_2, (d) ACC@DOX.Fe^{2+}-CaSi-PEG-N_3 and (e) ACC@DOX.Fe^{2+}-CaSi-PAMAM-FA/mPEG. The peak at 877.9cm^{-1} confirmed the successful construction of the $CaCO_3$ nanostructure. After the coating of silica shells, a new peak has appeared at 1086.7cm^{-1}, which was due to the stretching vibration of the Si-O bond. The silica coated ACC further reacted with APTES and resulted in the emergence of a new peak at 1656.2cm^{-1}, which confirmed the successful grafting of amine groups. Subsequently, the amine-modified nanoparticles were grafted with PEG-N_3 and two new peaks appeared at 2110.0cm^{-1} and 2875.0cm^{-1}, which correspond to the azide and methylene groups on the PEG-N_3, respectively. Eventually, after the conjugation of PAMAM-FA via click reactions, the azide peaks has disappeared as they were consumed during the reaction. Instead, two new peaks emerged near 1658.7cm^{-1}, which was assigned to the amine groups on the folate moiety. Additionally, another two peaks have appeared at 1499.3cm^{-1} and 1430.7cm^{-1}, which also correspond to the aromatic rings of attached folate moieties. **E**: Fluorescamine spectra of the nanoparticles at different synthesis stages: ACC@DOX.Fe^{2+}-CaSi, ACC@DOX.Fe^{2+}-CaSi-NH_2, ACC@DOX.Fe^{2+}-CaSi-PEG-N_3, ACC@DOX.Fe^{2+}-CaSi-PAMAM-FA/mPEG, MMP-2- treated ACC@DOX.Fe2+-CaSi-PAMAM-FA/mPEG. **F**: Zeta potential changes of the nanoparticles at different synthesis stages: (I) ACC@DOX.Fe^{2+}-CaSi, (II) ACC@DOX.Fe^{2+}-CaSi-NH_2, (III) ACC@DOX.Fe^{2+}-CaSi-PEG-N_3, (IV) ACC@DOX.Fe^{2+}-CaSi-PAMAM-FA/mPEG, (V) MMP-2-treated ACC@DOX.Fe^{2+}-CaSi-PAMAM-FA/mPEG. **G**: Zeta potential changes of ACC@DOX.Fe^{2+}-CaSi-PAMAM-FA/mPEG after incubation with various concentrations of MMP-2 for 12 h.

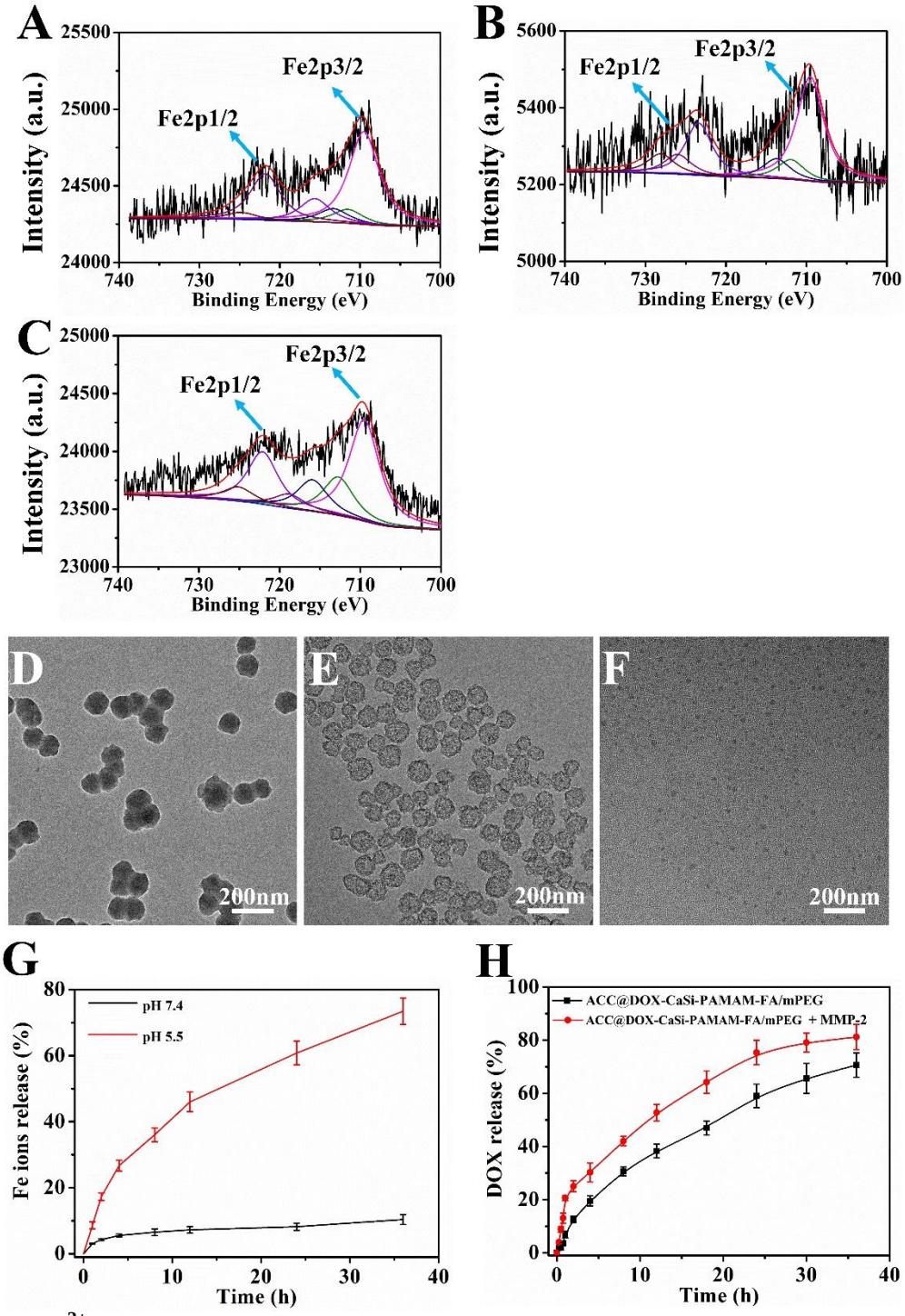

Fig. S4. Fe^{2+}-stabilizing effect and degradation-mediated drug release features of the ACC-based nanoformulation. (A-C) XPS spectra for the Fe2p regions of ACC@DOX.Fe^{2+}-CaSi-PAMAM-FA/mPEG incubated under incubation in (**A**) PBS, (**B**) cell medium, (**C**) serum for 24 h. (**D**) TEM image of ACC@DOX.Fe^{2+}-CaSi-PAMAM-FA/mPEG after incubated at pH7.4 for 24h. (**E**) and (**F**) are the TEM images of ACC@DOX.Fe^{2+}-CaSi-PAMAM-FA/mPEG after incubating at pH5.5 for 24h and 48 h, respectively. (**G**) The Fe release profiles from ACC@DOX.Fe^{2+}- CaSi-PAMAM-FA/mPEG under pH 7.4 and pH 5.5, as measured by ICP assay. (**H**) The DOX release profiles from ACC@DOX- CaSi-PAMAM-FA/mPEG and MMP-2-treated ACC@DOX- CaSi-PAMAM-FA/mPEG under pH 5.5.

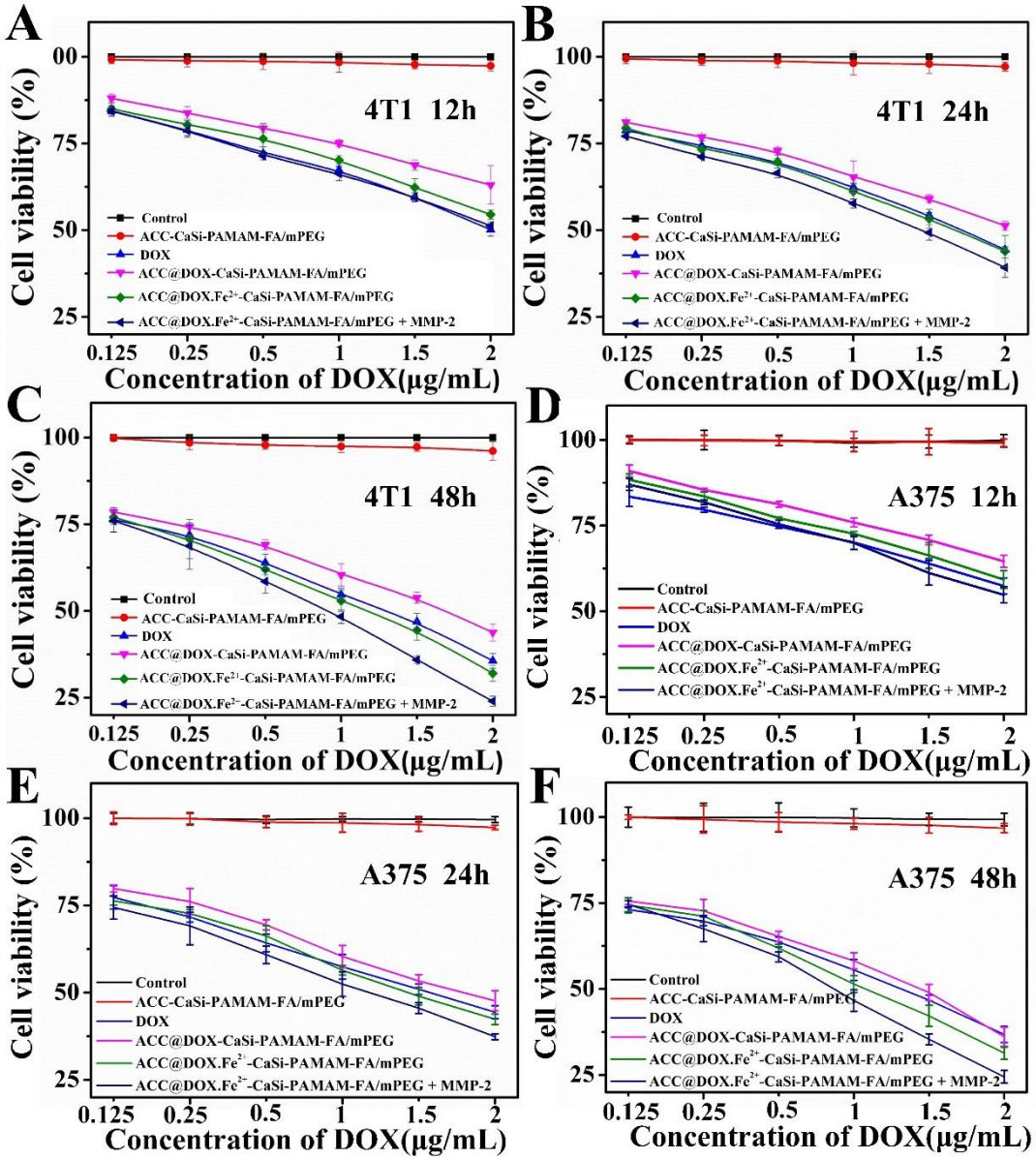

Fig. S5. Survival rates of 4T1 and A375 cells measured via MTT assay after incubation with PBS, ACC-CaSi-PAMAM-FA/mPEG, DOX, ACC@DOX-CaSi-PAMAM-FA/mPEG, ACC@ DOX.Fe^{2+}-CaSi-PAMAM-FA/mPEG and MMP-2 treated ACC@DOX.Fe^{2+}-CaSi-PAMAM -FA/mPEG. Panel **A/B/C** were 4T1 cells while panel **D/E/F** were A375 cells. The incubation periods were 12 h (**A, D**), 24 h (**B, E**) and 48 h (**C, F**), respectively.

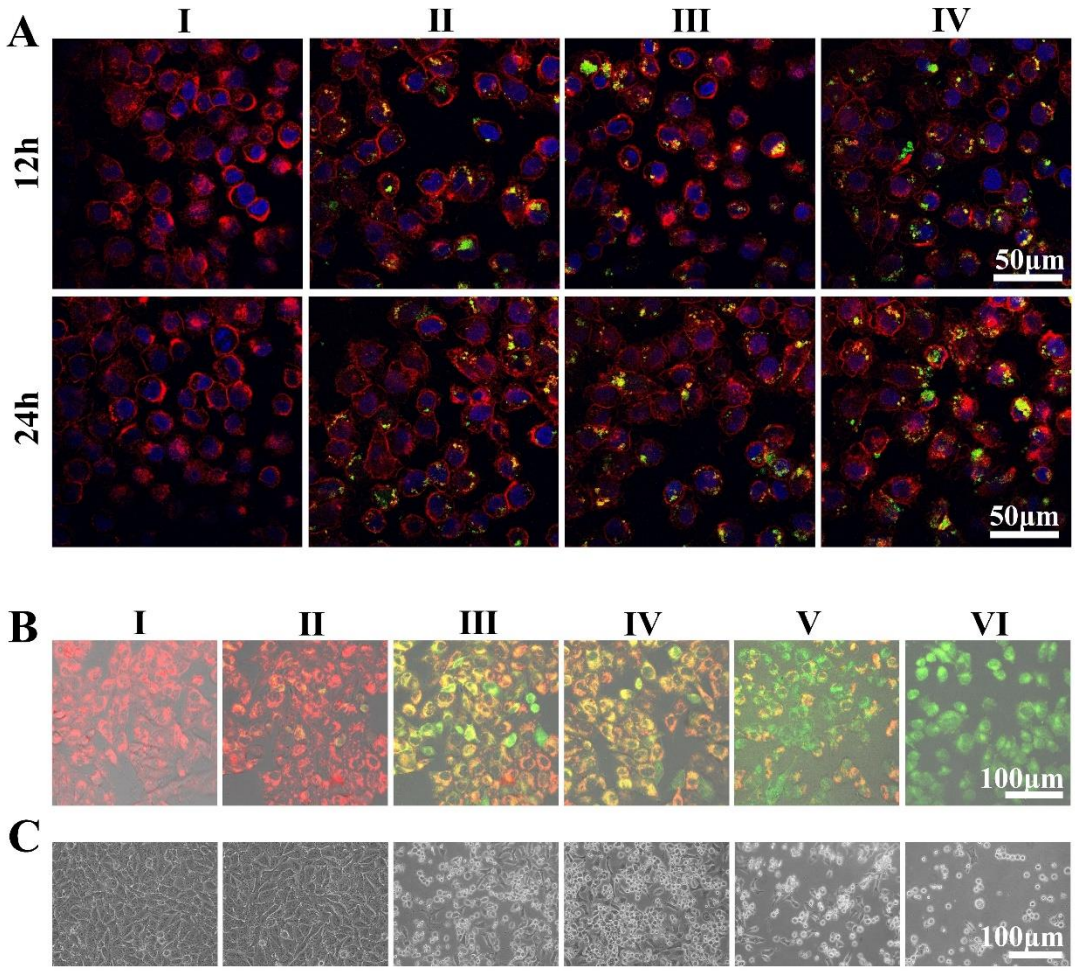

Fig. S6. CLSM and bright-field microscopic analysis of A375 cells after treatment with different samples. (**A**) CLSM images of A375 cells incubated with I: PBS, II: ACC@FITC-CaSi-PEG, III: ACC@FITC-CaSi-PAMAM-FA/mPEG and IV: MMP-2-treated ACC@FITC-CaSi-PAMAM-FA/mPEG for 12 h and 24 h. The blue, red and green colors indicate cell nucleus, cell membrane and the FITC-labelled nanoparticles, respectively. (**B**)CLSM observations on the changes in the mitochondrial membrane potential of A375 cells after incubation with PBS (I), ACC-CaSi-PAMAM-FA/mPEG (II), DOX (III), ACC@DOX-CaSi-PAMAM-FA/mPEG (IV) and MMP-2 treated ACC@DOX.Fe^{2+}-CaSi-PAMAM-FA/mPEG (V) for 24h. (**C**) Bright-field microscopy images of A375 cells after incubation with I: PBS, II: ACC-CaSi-PAMAM-FA/mPEG, III: DOX, IV: ACC@DOX-CaSi-PAMAM-FA/mPEG, V: ACC@DOX.Fe^{2+}-CaSi-PAMAM-FA/mPEG and VI: MMP-2 treated ACC@DOX.Fe^{2+}-CaSi-PAMAM-FA/mPEG for 24 h.

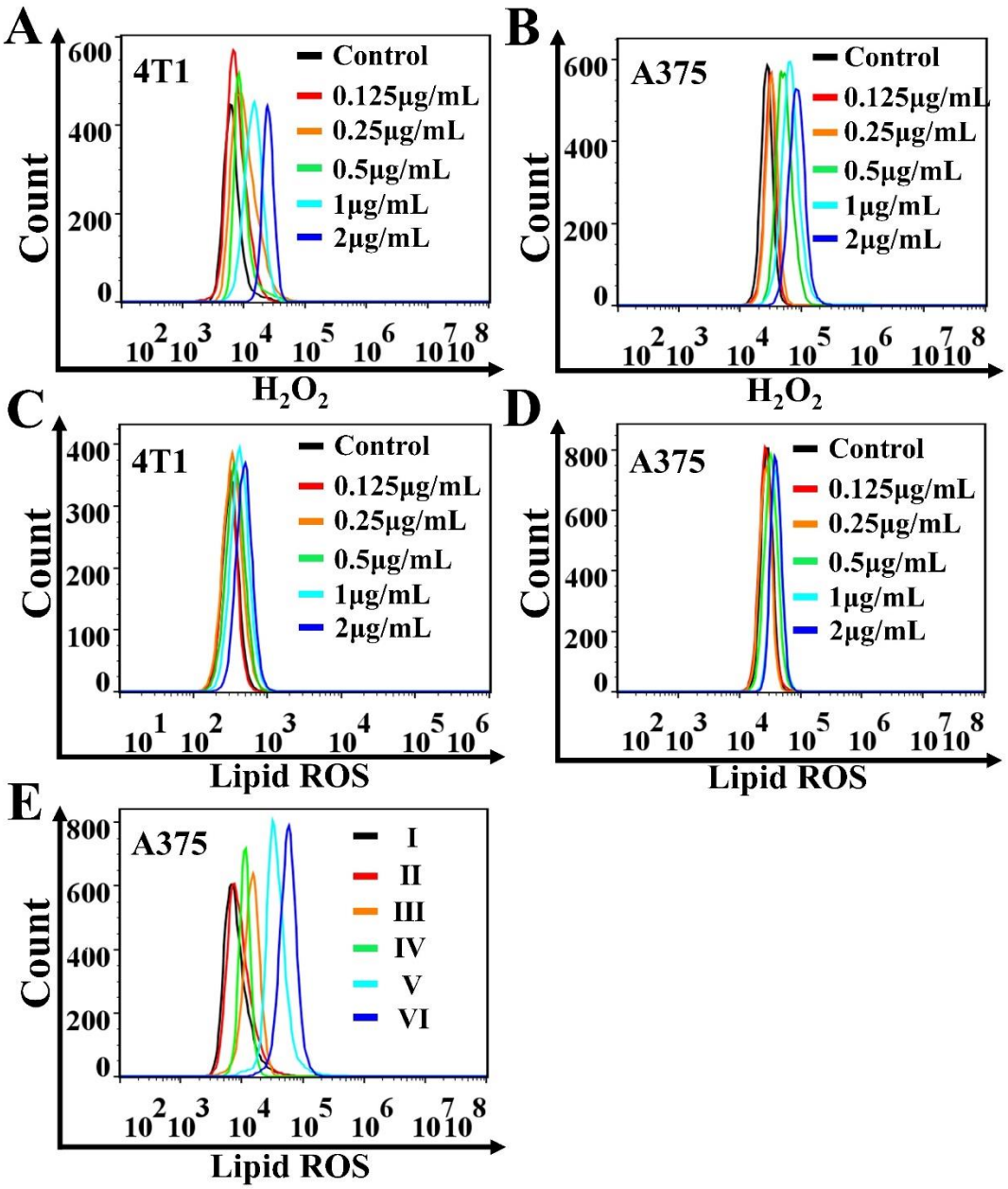

Fig. S7. Changes in the intracellular H_2O_2 and lipid ROS levels in 4T1 and A375 cells after different treatments. Panel (**A**) and (**B**) showed the flow cytometric analysis on the intracellular H_2O_2 levels in (**A**) 4T1 and (**B**) A375 cells after incubation with varied concentrations of DOX for 24 h. Panel (**C**) and (**D**) were the flow cytometric results on the intracellular lipoperoxide levels in 4T1 and A375 cells incubated with varied concentrations of DOX for 24 h, respectively. (**E**) Flow cytometric analysis on the intracellular lipoperoxide levels in A375 cells incubated with I: PBS, II: ACC-CaSi-PAMAM-FA/mPEG, III: DOX, IV: ACC@DOX-CaSi-PAMAM-FA/mPEG, V: ACC@DOX.Fe^{2+}-CaSi-PAMAM-FA/mPEG and VI: MMP-2 treated ACC@DOX.Fe^{2+}-CaSi-PAMAM-FA/mPEG for 24 h. The lipid ROS indicator in this test was BODIPY-C11.

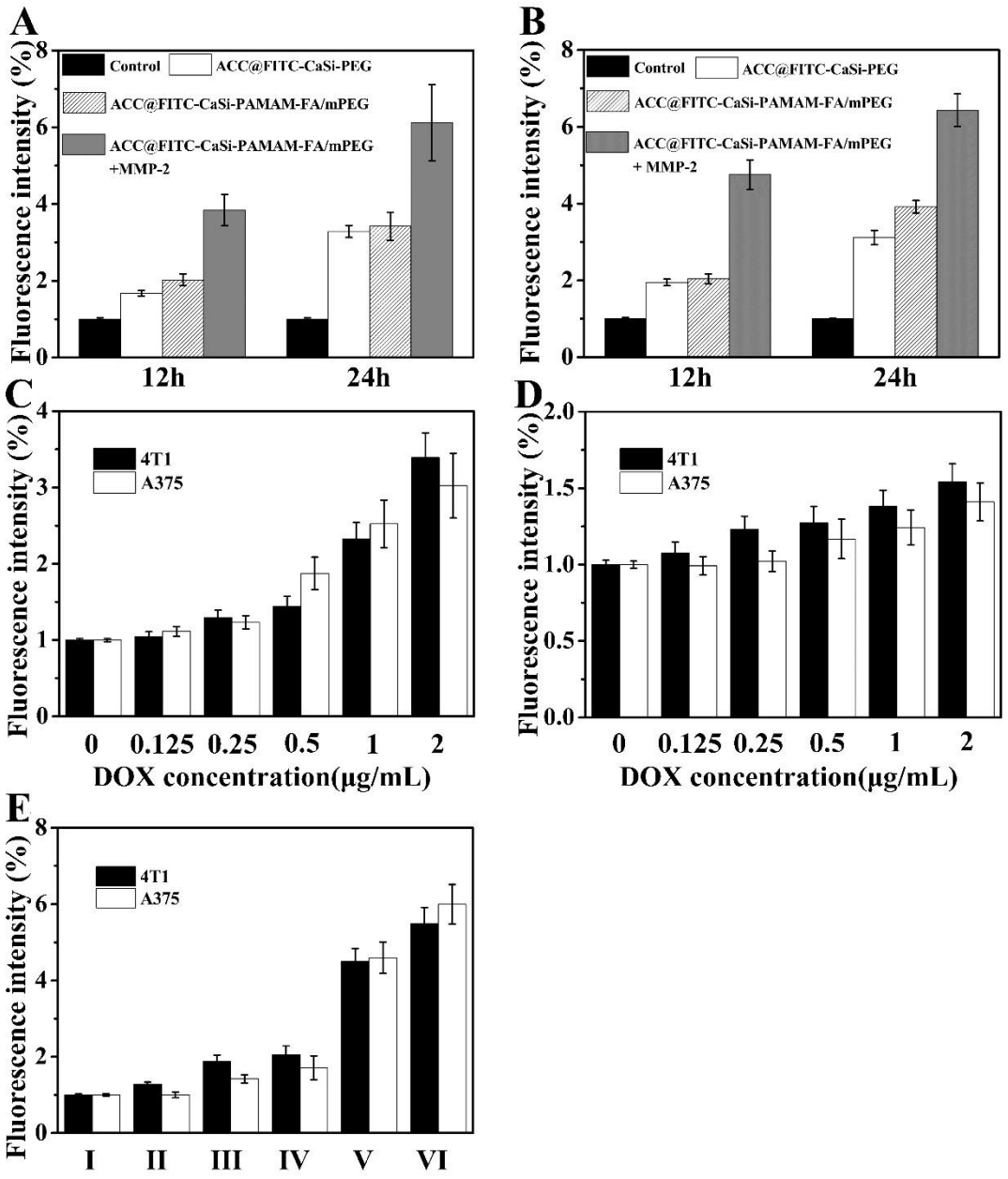

Fig. S8. Quantitative analysis on the uptake, H_2O_2 and lipid ROS levels in 4T1 and A375 cells after various treatments. Quantitative flow cytometric analysis on the FITC fluorescence of (**A**) 4T1 and (**B**) A375 cells after the incubation with I: PBS, II: ACC@FITC-CaSi-PEG, III: ACC@FITC-CaSi-PAMAM-FA/mPEG and IV: MMP-2-treated ACC@FITC-CaSi-PAMAM-FA/mPEG for 12 h and 24 h. **C**: Quantitative flow cytometric analysis on the intracellular H_2O_2 levels in 4T1 and A375 cells after incubation with varied concentrations of DOX for 24 h. (**D**) Flow cytometric analysis on the intracellular lipoperoxide levels in 4T1 and A375 cells incubated with varied concentrations of DOX for 24 h. (**E**) Flow cytometric analysis on the intracellular lipoperoxide levels in A375 cells incubated with I: PBS, II: ACC-CaSi-PAMAM-FA/mPEG, III: DOX, IV: ACC@DOX-CaSi-PAMAM-FA/mPEG, V: ACC@DOX.Fe^{2+}-CaSi-PAMAM-FA/mPEG and VI: MMP-2 treated ACC@DOX.Fe^{2+}-CaSi-PAMAM-FA/mPEG for 24 h.

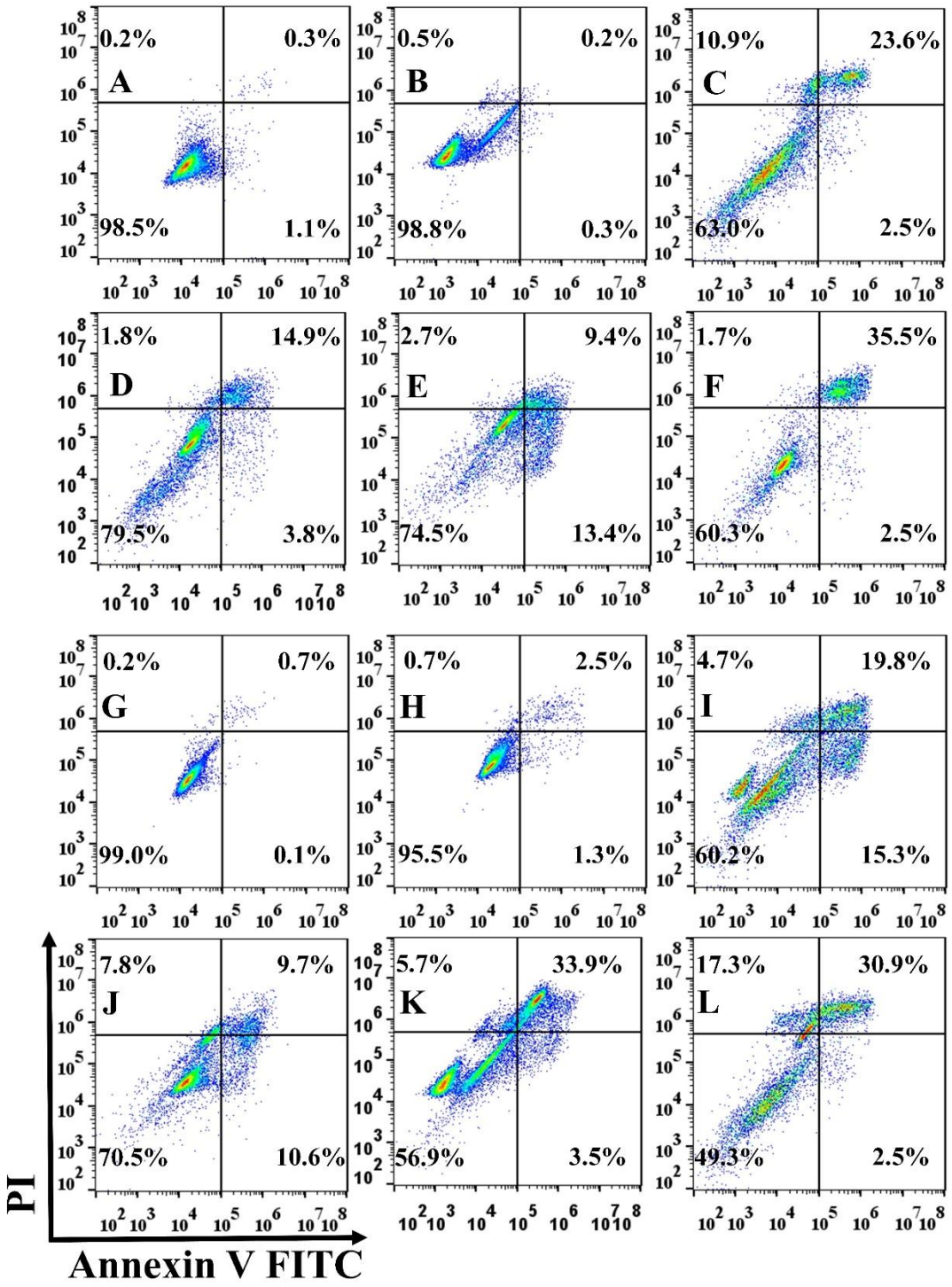

Fig. S9. Flow cytometric analysis on the apoptosis levels of A375 cells after different treatments. The incubation conditions are: (**A**) PBS, (**B**) ACC-CaSi-PAMAM-FA/mPEG, (**C**) DOX, (**D**) ACC@DOX-CaSi-PAMAM-FA/mPEG, (**E**)ACC@DOX.Fe^{2+}-CaSi-PAMAM-FA/mPEG and (**F**) MMP-2 treated ACC@DOX.Fe^{2+}-CaSi-PAMAM-FA/mPEG for 12 h. The corresponding results after 24 h were shown in panel **G-L**, respectively.

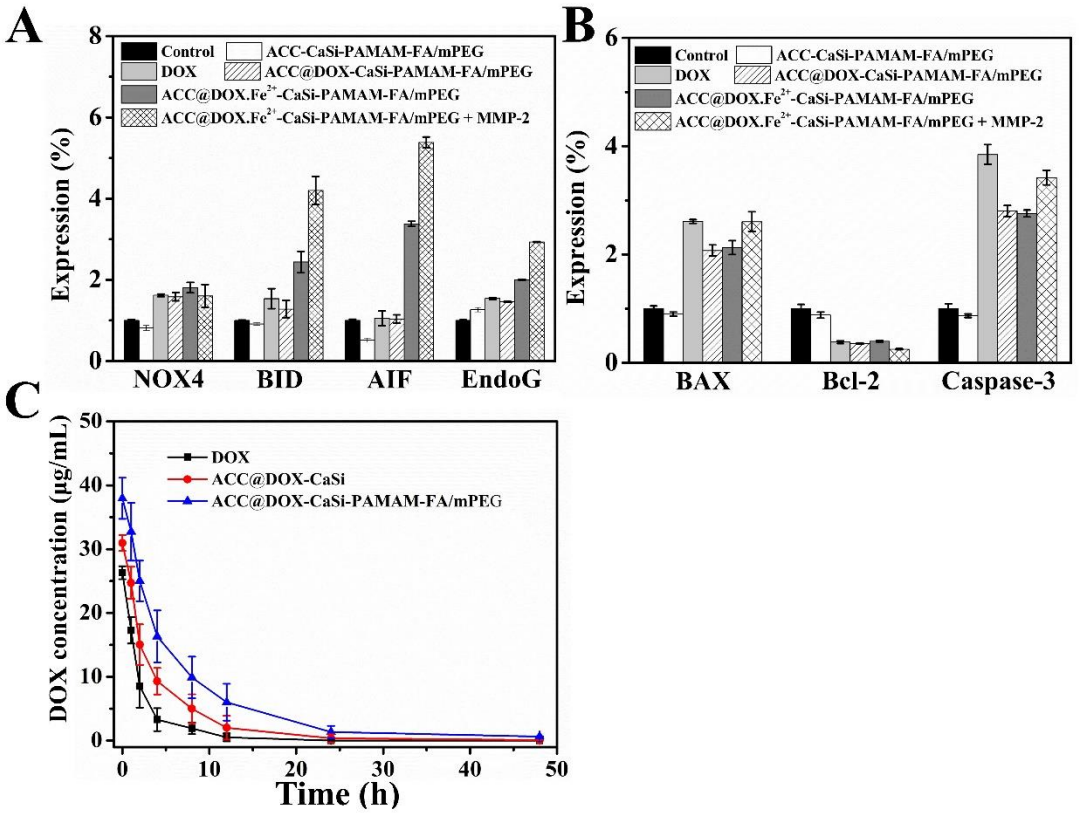

Fig. S10. Expression levels of key ferroptosis/apoptosis markers in vitro after different treatments and the blood stability of the nanoformulation in vivo. A-B: Quantitative analysis of the western blot results on the expression levels of ferroptosis and apoptosis markers in 4T1 cells after incubation with PBS, ACC-CaSi-PAMAM-FA/mPEG, DOX, ACC@DOX-CaSi-PAMAM-FA/mPEG and MMP-2 treated ACC@DOX.Fe^{2+}-CaSi-PAMAM-FA/mPEG for 24 h. **C**: Changes in the blood concentration of DOX, ACC@DOX-CaSi, ACC@DOX-CaSi-PAMAM-FA/mPEG in mouse over time (n=3). All samples were administered via intravenous injection.

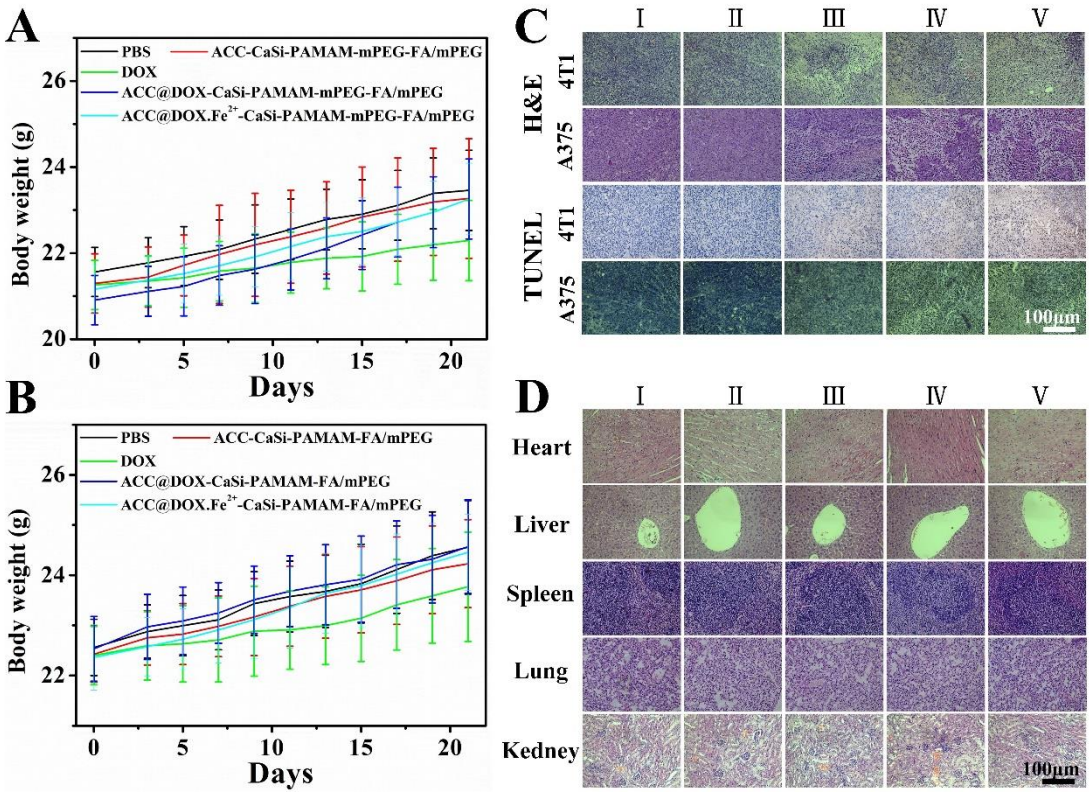

Fig. S11. Body weight changes of mice after different treatments and the corresponding histological analysis. A-B: Changes in the average body weight of tumor-bearing mice through the 21-day treatment period, which were recorded every 2 days (A: 4T1, B: A375). **C**: Histological analysis of the tumor slices under after H&E and TUNEL staining. I: PBS, II: ACC-CaSi-PAMAM-FA/mPEG, III: DOX, IV: ACC@DOX-CaSi-PAMAM-FA/mPEG and V: ACC@DOX.Fe^{2+}-CaSi-PAMAM-FA/mPEG. **D**: Histological analysis of the major organs (heart, liver, spleen, lung, kidney) extracted from 4T1-tumor bearing mice after the 21-day treatment, for which the organ slices were processed for H&E staining. I: PBS, II: ACC-CaSi-PAMAM-FA/mPEG, III: DOX, IV: ACC@DOX-CaSi-PAMAM-FA/mPEG, V: ACC@DOX.Fe^{2+}-CaSi-PAMAM-FA/ mPEG.